DEVELOPMENT OF PEGylated SILK FIBROIN NANOPARTICLES FOR DRUG DELIVERY SYSTEMS

Andreea-Cristina ION[1], Ionut-Cristian RADU[2], Eugeniu VASILE[3], Elena Iuliana BIRU[4], Ariana HUDITA[5], Bianca GALATEANU[6], Horia IOVU[7], Catalin ZAHARIA[8*]

The aim of this research consists in the development of drug delivery formulations based on silk fibroin and polyethylene glycol nanoparticles. The obtained nanoparticles were characterized by FTIR-ATR and RAMAN. The morphological investigation and size distribution profile of the nanoparticles were performed by scanning electron microscopy (SEM) and dynamic light scattering (DLS). Drug release behavior for 5-fluorouracil-loaded PEGylated silk fibroin nanoparticles was investigated.

Keywords: silk fibroin, polyethylene glycol, nanoparticles, 5-FU, drug delivery

1. Introduction

During the last several decades extensive reseach has been made on drug delivery systems (DDSs). The development approaches were set to improve the drug solubility, to achieve specific control drug release targeting or prolong circulating time. Furthermore, the toxicity reduction or immunogenicity minimazation were aims to be achieved [1-3]. Recently, the therapeutics efficacy optimization was proposed to be achieved by multiple drug administration and release, in a controlled manner in comparison with classic procedures. Both synthetic and natural polymers have been used for drug delivery applications [4-6]. A large part of the scientific community considers nanotechnology as the

[1] PhD student, Advanced Polymer Materials Group, University POLITEHNICA of Bucharest, Romania, e-mail: i.andreeacristina@yahoo.com
[2] PhD, Advanced Polymer Materials Group, University POLITEHNICA of Bucharest, Romania, e-mail: radu.ionucristian@gmail.com
[3] PhD, University POLITEHNICA of Bucharest, Romania, e-mail: eugeniuvasile@yahoo.com
[4] PhD, Advanced Polymer Materials Group, University POLITEHNICA of Bucharest, Romania, e-mail: iuliana.biru@yahoo.com
[5] PhD, Department of Biochemistry and Molecular Biology, University of Bucharest, Romania, e-mail: arianahudita@yahoo.com
[6] PhD, Department of Biochemistry and Molecular Biology, University of Bucharest, Romania, e-mail: bianca.galateanu@bio.unibuc.ro
[7] Prof., Advanced Polymer Materials Group, University POLITEHNICA of Bucharest, Romania, e-mail: horia.iovu@upb.ro
[8] Prof., Advanced Polymer Materials Group, University POLITEHNICA of Bucharest, Romania, e-mail: zaharia.catalin@gmail.com

science key of the new millennium. Nanotechnology represents the science way where the material is controlled and manipulated at atomic and molecular dimensions (1-100 nm). In this dimension range acts a number of biological entities essential for the living organisms processes. Numerous specific carriers with these sizes have been developed: nanoparticles, dendrimers, nanotubes [7]. Nanoparticles are colloidal particles which take the form of nanocapsules or nanospheres. They have a role in active principles targeting and controlled release (drugs, hormones, vitamins, etc.).

The nanoparticle surface chemistry is a very important aspect in drug delivery targeting. After bloodstream reaching, generally, no surface modified (conventional) and negatively charged nanoparticles can be rapidly opsonized and massively cleared by the fixed macrophages. It is well known that the reticuloendothelial system (RES) is a major obstacle for the active targeting. The biological system has ability to recognize and remove these systems from systemic circulation [8-11]. The main used material in this reseach, silk, is a natural polymeric material. Natural silk is a hardened glandular secretion of the silkworms larva from species such as *Bombyx Mori*. The larva deposits the fiber in the form of a cocoon [12-13]. Natural silk is composed of two major proteins, fibroin and sericin. Silk fibroin (SF) is the simplest structural protein in terms of amino acid composition and the sequence between them. It consists mainly of glycine, alanine and serine in a ratio of 3: 2: 1. These amino acids represent approximately 60% of the fibroin crystalline domains. These domains have the following aminoacids sequence: Gly-Ala-Gly-Ala-Gly-Ser-Gly-Ala-Gly-Ala-Gly-Ser. The SF chains also contain amino acids with bulky and polar side chains such as tyrosine, valine or acidic amino acids [14-16]. The highly ordered amino acids can form anti-parallel β-sheets which have high influence in the fiber stability and mechanical properties. These crystalline β-sheets essentially crosslink the protein through strong intra- and inter-molecular hydrogen bonds. Furthermore, strong van der Waals interactions between the methyl groups and opposing side hydrogen allow inter-sheet stacking in the crystals. A thermodynamically stable structure is generated which assure robust mechanical properties [17-18]. Silk fibroin protein can improve the cells adhesion and proliferation taking into account its biocompatibility [19-22]. Thus, fibroin offers chemical modification and crosslinking possibility in order to design SF-based nanoparticles as a promising drug delivery system [23]. Another important polymer with a great potential in therapeutic applications for controlled release of drugs is Polyethylene glycol (PEG). The PEG addition to protein nanoparticles increases the chance of tumoral cells to be reached. Thereby, the drug carriers surface modification minimizes the opsonization effect [24-26]. Regarding silk and PEG interactions, the silk fibroin nanoparticles are coated with PEG due to its hydrophilic nature. Polyethylene glycol molecules induce silk conformational changes by forming β-

sheet stacks. This process is an exceptional way to obtain water insoluble microspheres. The procedure can be achieved by nanoprecipitation in a water-miscible organic solvent to obtain PEGylated nanoparticles [27-29].

This study focuses on the development of polymeric nanocarriers based on silk fibroin chemically modified with PEG as a drug delivery approach. The particle size, chemistry and properties adjustment by PEG modification was employed to improve the therapeutic efficacy of the encapsulated drugs.

2. Experimental

2.1. Materials

The following materials were used in the experimental study: *Bombyx mori* cocoons provided by SC Sericarom SA, sodium carbonate (Na_2CO_3) and sodium bicarbonate ($NaHCO_3$) supplied from Chimopar Trading SRL, sodium dodecyl sulfate provided by Merck and lithium bromide (LiBr) purchased from Honeywell. Other materials were N- hydroxysuccinimide (NHS), poly(ethylene glycol) diacrylate (PEG diacrylate) with an average molecular weight (M_n) of 700 g/mol, tetra(ethylene glycol) diacrylate (TEG diacrylate) with an average molecular weight of 302.32 g/mol and potassium persulfate (KP) provided by Sigma-Aldrich.

2.2. Preparation of silk fibroin solution

Bombyx mori cocoons were degummed by boiling in an aqueous solution containing 0.02 M Na_2CO_3, $NaHCO_3$ and sodium dodecyl sulfate for 30 minutes in order to remove the sericin and other impurities [30]. This procedure was repeated three times. The last step consisted of silk fibroin fibers washing with distilled water for surfactant removal. The purified fibroin was dried at 40 ℃ for 24 hours. Silk fibroin solution was prepared by silk fibroin dissolution in a 9.3 M LiBr aqueous solution at 60 ℃. The resulted solution of 5% concentration was dialyzed against water for 5 days for the ions removal. The procedure was performed in a cellulose dyalisis membrane with frequent water change.

2.3. Preparation of silk fibroin-acrylic acid solution

In order to obtain the silk fibroin-acrylic acid solution, 10 ml of 5% silk fibroin (SF) solution and 5 mg of N-hydroxysuccinimide (NHS) were mixed until NHS dissolution. Then 0.475 ml of acrylic acid was added. This solution was mixed at 700 rpm for 4-6 h, then washed with distilled water. The obtained precipitate was dissolved in 9.3 M LiBr aqueous solution at 60 ℃. SF-acrylic acid solution was dialyzed for 5 days with frequent water change.

2.4. Preparation of SF-PEG solutions

Two different types of PEG were used for this experiment: Poly(ethylene glycol) diacrylate and Tetra(ethylene glycol) diacrylate. For each type of PEG

diacrylate, two aqueous solutions were prepared (25 wt. %). These solutions contain poly(ethylene glycol) diacrylate/ Tetra(ethylene glycol) diacrylate with potassium persulfate as initiator (0.07-0.14 wt.% versus total mixture volume) along with SF-acrylic acid solution. The differences between "silk fibroin-PEG solutions" (Table 1) are found in the volumetric concentration of SF-acrylic acid solution in ratio with PEG diacrylate/TEG diacrylate solutions.

Table 1

Composition of SF-PEG samples

SAMPLE NAME	SF-ACRYLIC ACID	POLY(ETHYLENE GLYCOL) DIACRYLATE AND KP SOLUTION	TETRA(ETHYLENE GLYCOL) DIACRYLATE AND KP SOLUTION
SILK FIBROIN-PEG SAMPLE 1 (11.1)	3 ML	1 ML	-
SILK FIBROIN-PEG SAMPLE 2 (11.2)	2 ML	2 ML	-
SILK FIBROIN-PEG SAMPLE 3 (22.1)	3 ML	-	1 ML
SILK FIBROIN-PEG SAMPLE 4 (22.2)	2 ML	-	2 ML

2.5. Preparation of SF-PEG nanoparticles

The nanoparticles were obtained by nanoprecipitation method. Briefly, the silk fibroin-PEG samples (4 ml) were added dropwise in a water-miscible organic solvent, acetone, under high stirring for 1 minute at room temperature. The volumetric ratio between SF-PEG solution and non-solvent was set to 1/9 (v/v).The prepared suspension of nanoparticles was heated at 60 ºC to induce nanoparticles crosslinking.

2.6. Methods

A Fourier-transform infrared Bruker Vertex 70 FT-IR spectrophotometer was used to confirm the structure of the SF-acrylic acid and SF-PEG particles. The spectrophotometer used 32 scans and a resolution of 4 cm^{-1} in mid-IR region 4000-600 cm^{-1}. Spectra of SF, acrylic acid and SF-acrylic acid PEG diacrylate, TEG diacrylate and the nanoparticles were recorded to evaluate the structure and chemical modification.

RAMAN spectrometry along with FT-IR are complementary vibrational spectrometry techniques which allow the study of the chemical composition and molecular structure of this biopolymers. Raman spectra were taken on a DXR model, from Thermo Fisher Scientific (Wisconsin, USA). The excitation laser wavelength used was 785 nm using a laser power of 10 % [31]. The Raman spectra were recorded in the range of 3200–200 cm^{-1}. The ratio between S/N was 100.

In order to determine the particles size distribution profile in solution, Dynamic Light Scattering (DLS) using a Malvern Zetasizer Nano (Malvern, model ZEN5600, United Kingdom) was used.

Morphological information including nanoparticles size and shape were obtained by the scanning electron microscopy (SEM) analysis of the gold-coated nanoparticles. The analysis was performed on a Quanta Inspect F SEM device equipped with a field emission gun (FEG) with a resolution of 1.2 nm and with an X-ray energy dispersive spectrometer (EDS).

Drug release curves for 5-FU loaded silk fibroin PEGylated nanoparticles were obtained by *in vitro* release assessment. Nanoparticles loaded with the active substance were added to a tubular cellulose membrane and immersed in a flask with 40 ml of phosphate-buffered saline (PBS, pH 7.45). The flask was incubated in an orbital mixer (Benchmark Scientific) at 300 rpm and 37.0 ± 0.5 ° C. For one hour, at every 15 minutes, a volume of 5 ml of PBS with released 5-FU was collected and evaluated by UV-VIS spectroscopy with a UV-3600 Shimadzu UV-VIS-NIR spectrophotometer. After one hour, the procedure was repeated every 30 minutes for 5 hours. Then, samples were collected at every hour until the experiment ends. For each collected sample, an equivalent amount of fresh PBS was added to maintain a constant volume of release medium.

3. Results and discussion

3.1. Pathaway to nanoparticles preparation

The pathway and mechanism from acrylic acid, silk fibroin and PEG to nanoparticles formation is shown in Fig. 1. Firstly, the carboxylic group from acrylic acid is activated with N-Hydroxysuccinimide (NHS). Then, the activated acrylic acid reacts with silk fibroin through hydroxyl groups from 2 silk fibroin amino acids: serine (11.9 %) and threonine (1 %) [33]. The hydroxyl groups react with the carboxylic group to form esters. Finally, the carbon-carbon double bonds from PEG/TEG diacrylates, react with the carbon-carbon double bonds from modified SF-acrylic acid. In the last step, acetone was added to induce nanoparticles formation, and heating at 60 ℃ induced further crosslininking of SF-PEG nanoparticles.

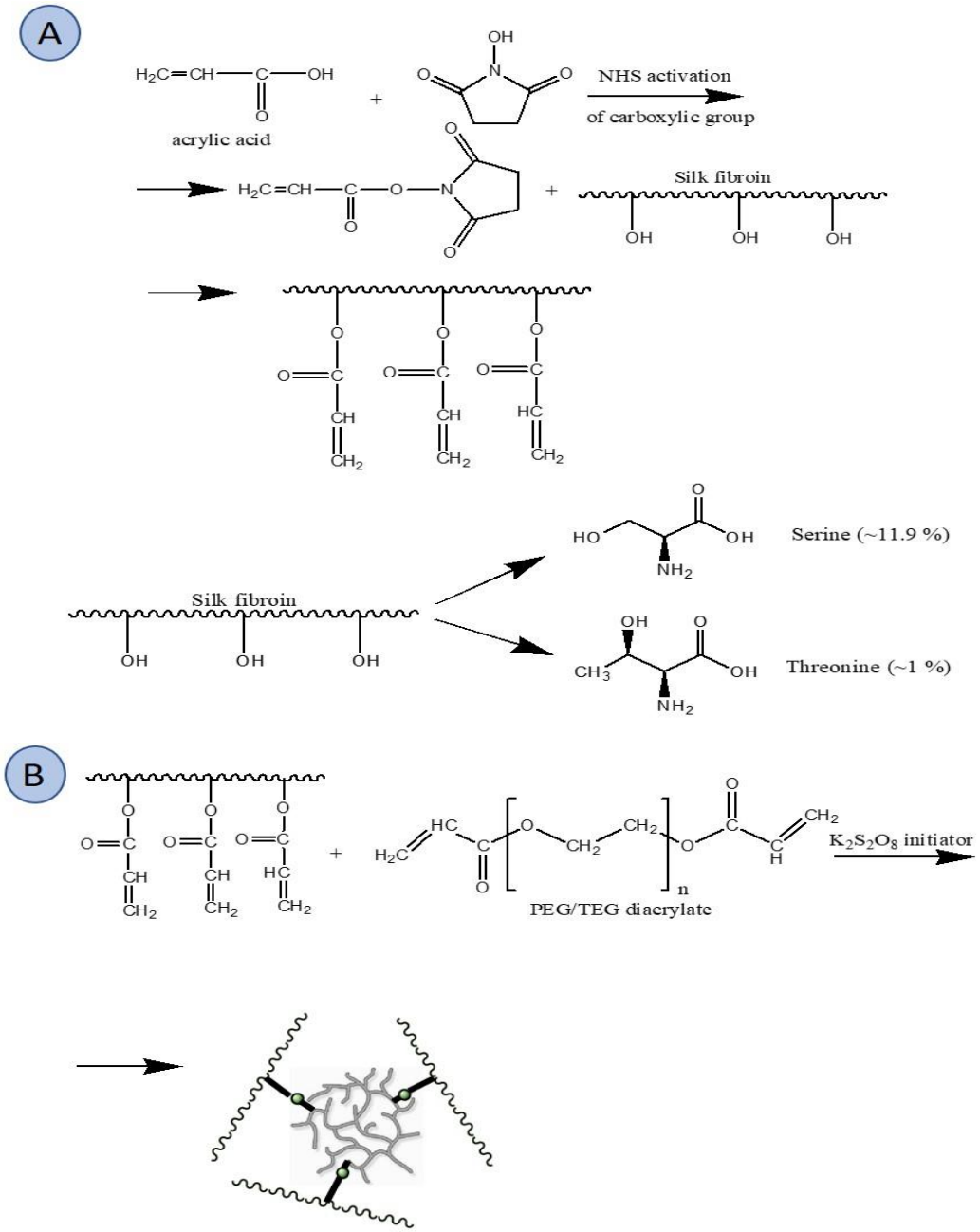

Fig. 1. Pathaway and mecahnism of SF-PEG nanoparticles formation: A) SF-acrylic acid; B) SF-acrylic acid and PEG

3.2. FTIR spectroscopy

FTIR spectra showed the main characteristic peaks for SF, Acrylic acid and SF-Acrylic acid compound (Fig. 2). In SF spectrum, peaks around 3287 cm^{-1} are attributed to hydroxyl stretching vibration, peaks in the range 3080-3075 cm^{-1}

are attributed to N-H (amide IV) stretching vibration and peaks in the range 2978-2072 cm^{-1} corresponded to carbon-hydrogen asymmetric stretching. Next peaks, amide I for carbonyl stretching vibration at 1628 cm^{-1}, amide II for nitrogen-hydrogen deformation vibration at 1521 cm^{-1} and amide III for carbon-nitrogen stretching vibration at 1234 cm^{-1} are shown in the spectrum.

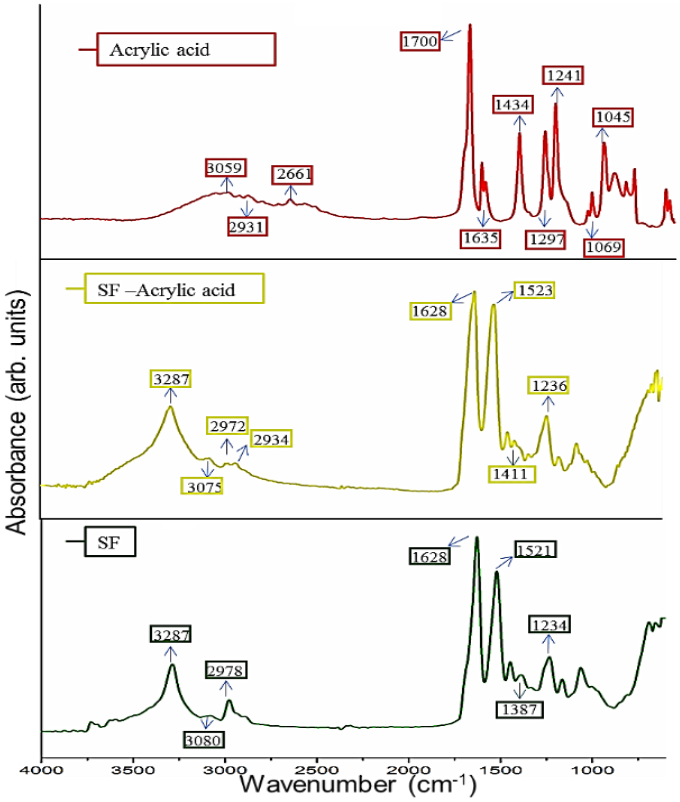

Fig. 2. ATR-FTIR spectra of SF, Acrylic acid and SF-acrylic acid

SF-Acrylic acid showed a similar spectrum with SF spectrum. There are few differences between the spectra: two new signals, one at 1411 cm^{-1} and other at 1052 cm^{-1} can be observed. The signal at 1411 cm^{-1} was assigned to CH_2=CH- deformation from acrylic acid and the signal at 1052 cm^{-1} corresponded to the ester group from acrylic acid. The chemical interaction between silk fibroin and acrylic acid was highlighted by these two peaks. Furthermore, the area attributed to the amide IV (N-H stretching vibration) increased in the case of modified SF-Acrylic acid. This approach may be explained by the new contribution of carbon-hydrogen stretching vibration within carbon double bond from acrylic acid moiety.

In order to evaluate the silk fibroin modification with acrylic acid a quantitative analysis of FTIR spectra was performed. Using the equation below, the contribution of C-H from CH_2=CH- groups was determinated. The equation

revealed that amide IV area (N-H stretching vibration) was about 29 % higher in the SF-acrylic acid spectrum with respect to unmodified silk fibroin. The value was considered in ratio to the constant peak, amide II, in order to show only the contribution of carbon double bond from acrylic acid moiety.

$$\% = 1 - \frac{\frac{A(3110-3030)}{A(1591-1483)} of\ SF}{\frac{A(3110-3030)}{A(1591-1483)} of\ modified\ SF}$$

where % corresponds to the contribution of the C-H groups from the double bonds, A(3110-3030) is area of 3075 cm^{-1} signal attributed to amide IV (N-H stretching vibration) from SF-Acrylic acid and SF spectra; A(1591-1483) is area of 1523/1521 cm^{-1} signal from SF-Acrylic acid and SF spectra attributed to amide II (N-H deformation vibration.

The silk fibroin characteristic peaks are also present into PEGylated samples. Fig. 3 revealed the FTIR spectra of Poly(ethylene glycol) diacrylate (11),

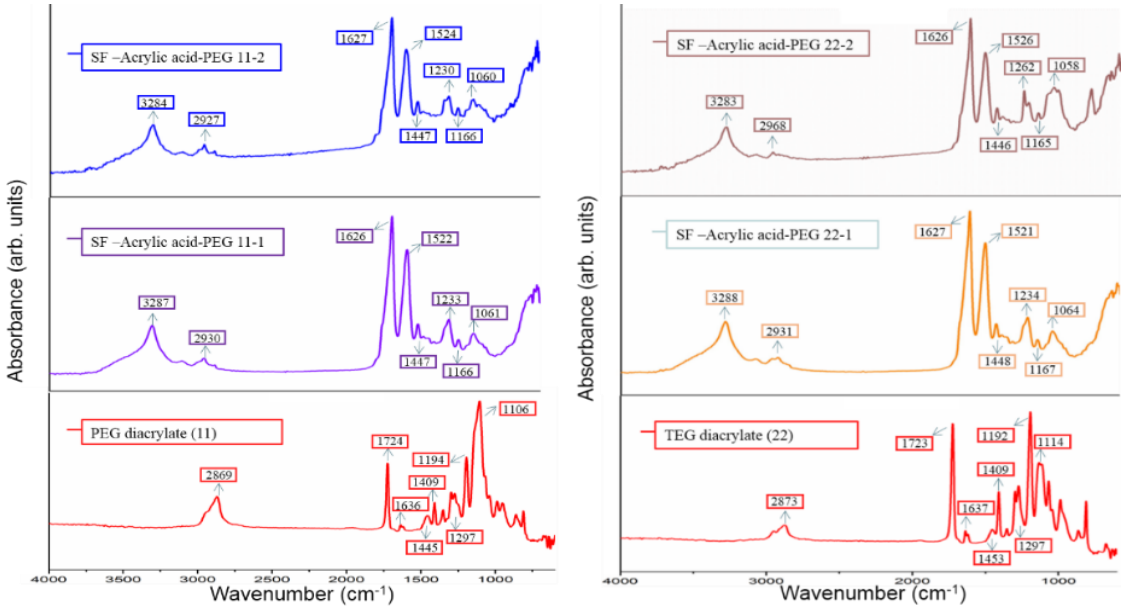

Fig. 3. ATR-FTIR spectra of PEGylated SF nanoparticles

Tetra(ethylene glycol) diacrylate (22) and the PEGylated silk fibroin compounds. The chemical modification consists in splitting of amide III (stretching C-N) into two different peaks according to concentration of PEG formulations. Another important aspect is that no signals for C=C groups at 1411 cm^{-1} appeared, as it was revealed in SF-Acrylic acid spectrum. This approach may demonstrate the reaction between carbon-carbon double bonds from PEG with

carbon-carbon double bonds from modified SF-Acrylic acid. This achievement represents a pathway for a directly crosslinked structure by the contribution of both synthetic and natural polymers.

3.3. RAMAN spectroscopy

The physico-chemical investigation was also carried out by RAMAN analysis. Fig. 4 reveals the main peak of SF and modified SF (SF-Acrylic acid). SF spectrum presented four main peaks: in the region 2937 cm^{-1} a peak attributed to the carbon-hydrogen stretching; in the region 1667 cm^{-1} a peak specific to carbonyl group and a peak in the region 1453/1388 cm^{-1} attributed to the carbon-hydrogen bending. The modified SF spectrum revealed a new peak at 1234 cm^{-1} which can be the amide III contribution (carbon-nitrogen stretching) from the native fibroin. Two more peaks at 1173 cm^{-1} and 1085 cm^{-1} can be attributed to the ester group and carbon oxygen stretching from the acrylic acid bound within fibroin backbone. Other peaks can be seen under 1000 cm^{-1} region and they can be attributed to the carbon-carbon stretching from the acrylic acid moiety.

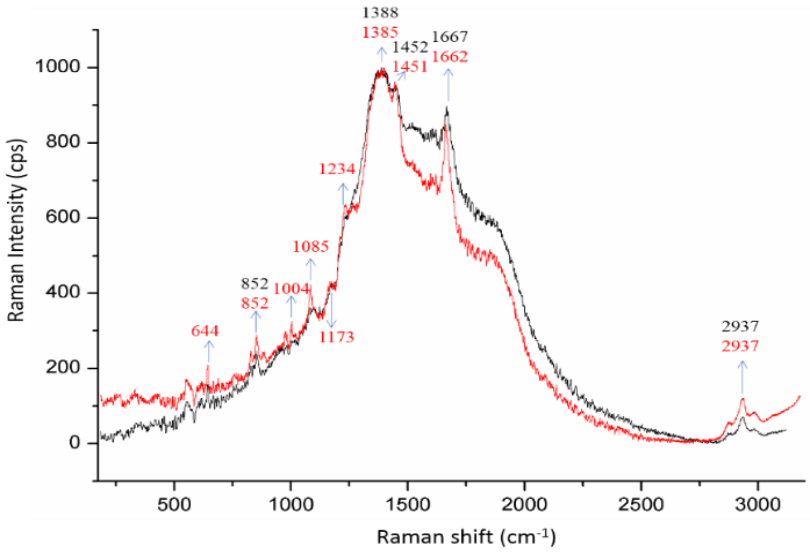

Fig. 4. RAMAN spectra of SF (black) and SF-Acrylic acid (red)

3.4. Dynamic light scattering (DLS)

The of SF-PEG nanoparticles size distribution profile in solution was evaluated by Dynamic light scattering (DLS, Fig. 5). Crosslinked and uncrosslinked SF-PEG samples were analyzed to reveal the PEG contribution over nanoparticles size. Bigger particles size was shown for crosslinked nanoparticles in comparison with un-crosslinked samples. This fact can be attributed to the swelling behavior of a crosslinked structure. Considering the

analysis in the aqueous solution, there is a favourable environment for the SF-PEG network to swell.

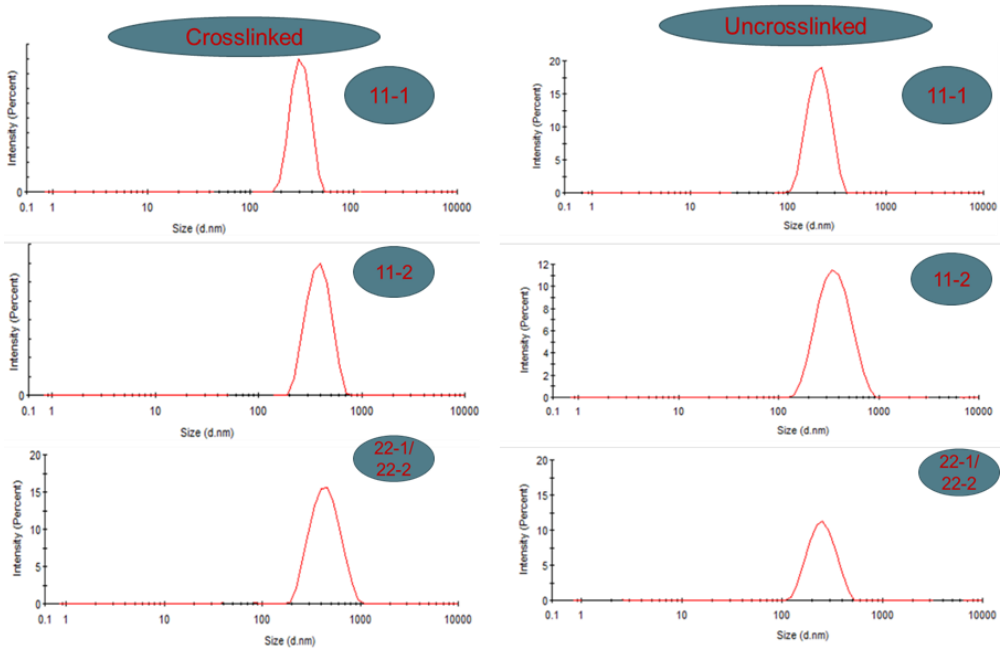

Fig. 5. DLS spectra of crosslinked and uncrosslinked samples of silk fibroin-PEG solution 1 (11-1), silk fibroin-PEG solution 2 (11-2) and silk fibroin-PEG solutions 3 and 4 (22-1/22-2)

In the case of modified SF with acrylic acid the generated structure can be considered as a physical network.

Table 2

Particle size of SF-PEG samples

	SAMPLE NAME	PARTICLE SIZE (NM)
CROSSLINKED	SILK FIBROIN-PEG SAMPLE 1 (11-1)	295 ±20
	SILK FIBROIN-PEG SAMPLE 2 (11-2)	380 ±20
	SILK FIBROIN-PEG SAMPLES 3 AND 4 (22-1/22-2)	390 ±20
UN-CROSSLINKED	SILK FIBROIN-PEG SAMPLE 1 (11-1)	220
	SILK FIBROIN-PEG SAMPLE 2 (11-2)	350
	SILK FIBROIN-PEG SAMPLES 3 AND 4 (22-1/22-2)	260

The hydrogen bonds and rearrangement of the spatial conformation via random-to-β-sheets contributed to the physical network achievement. The PEG chemical

network contribution to the final nanoparticles network is essential because of balance increasing to a more hydrophilic nature. This fact certainly contributes to the nanoparticles swelling capacity and size increase. The samples with tetra(ethylene glycol) diacrylate 22-1 and 22-2 revelaed bigger particle size due to the fact that this type of PEG is more reactive than poly(ethylene glycol) diacrylate. A more reactive PEG generates a chemical network with a higher contribution to the final nanoparticles network and swelling behavior. In this case, the nanoparticles size was decided by the PEG reactivity to the detriment of the PEG molecules size.

3.5. Scanning Electron Microscopy (SEM)

PEGylated silk fibroin surfaces were visualized by SEM in terms of surface morphology and nanoparticles dimensions. Samples formulated with poly(ethylene glycol) diacrylate showed homogenous individualized nanoparticles but in a low number. A slight increase of nanoparticles dimensions can be observed between sample 11-1 and sample 11-2 (Fig. 6).

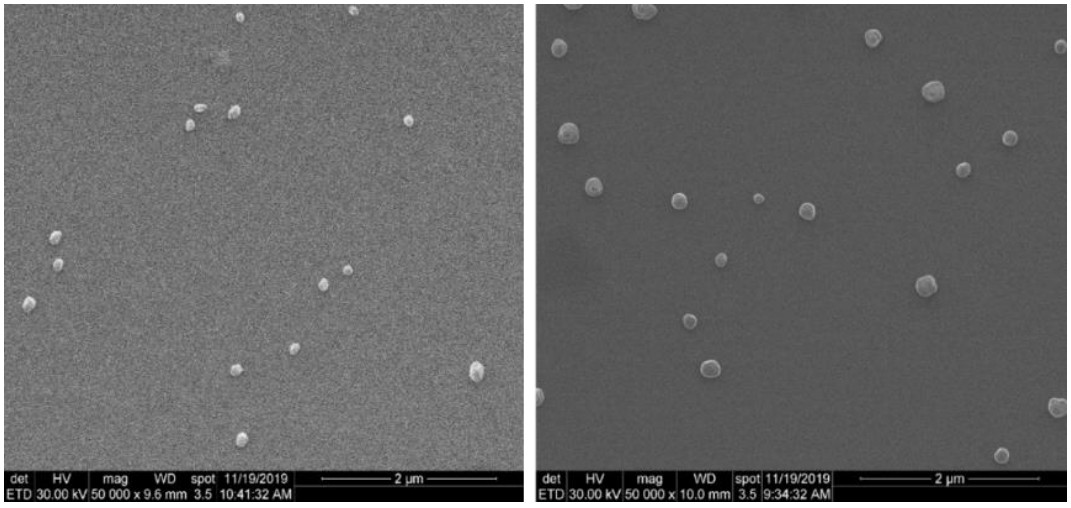

Fig. 6. SEM microphotographs of nanoparticles: silk fibroin-PEG sample 1 (11-1, left) and silk fibroin-PEG sample 2 (11-2, right)

Regarding samples formulated with tetra(ethylene glycol) diacrylate, nanoparticles have the tendency to agglomerate and stick together. According to the SEM images, smaller nanoparticles are highlighted with respect to DLS for the same formulation (Fig. 7). This aspect can be explained by the fact that in the case of DLS nanoparticles agglomerates were analyzed with negligible contribution of individualized nanoparticles. The real nanoparticle sizes were presented only by morphological investigation.

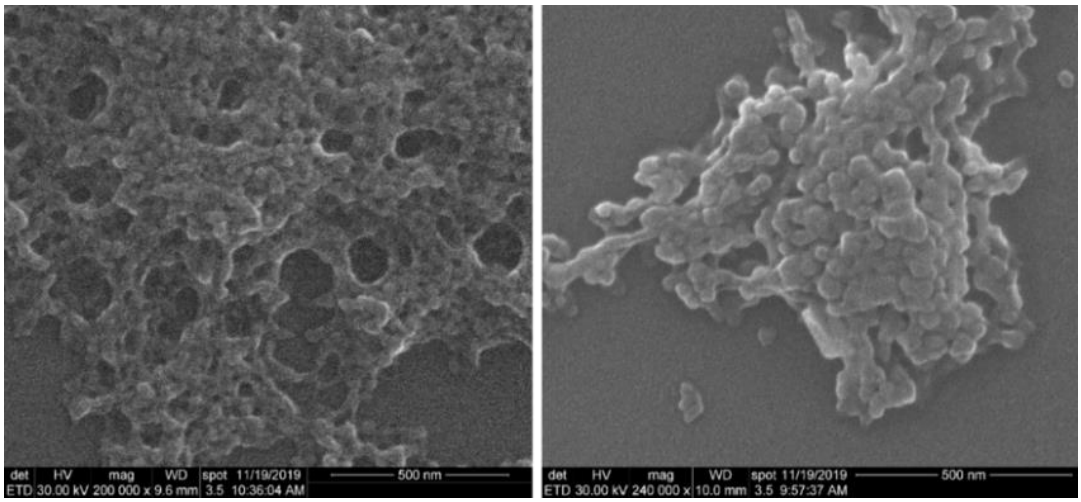

Fig. 7. SEM microphotographs of nanoparticles from silk fibroin sample 3 (22-1, left) and silk fibroin sample 4 (22-2, right)

3.6. Drug release behavior

Fig. 8 shows the release curve of SF-PEG samples loaded with 5-fluorouracil (5-FU). The 5-FU release was evaluated every 15 minutes for the first hour, every 30 minutes for the next two hours and finally 240 minutes after the beginning of the experiment.

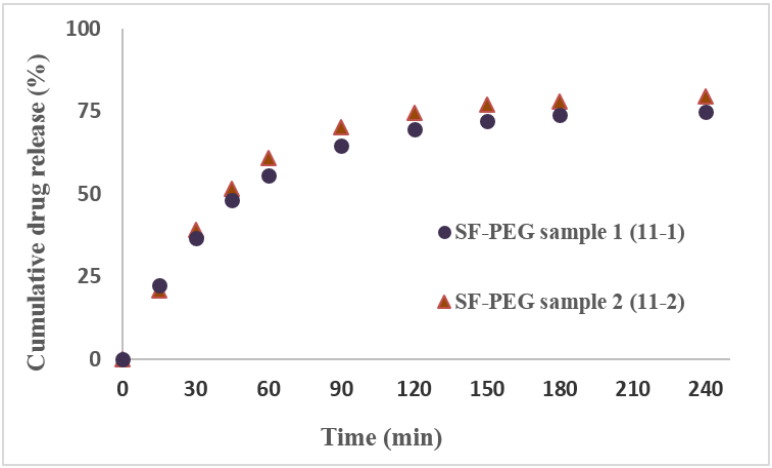

Fig. 8. 5-Fluorouracil release profiles from SF-PEG nanoparticles

A higher amount of drug is released from the polymeric nanoparticles into the PBS buffer in the first 60 minutes. This might be due to the kinetic forces which occur within the system as a result of aqueous media penetration of the polymer nanoparticles. Furthermore, the osmotic pressure enables the strong purge of 5-FU from nanoparticles. This linear-like profile changes afterwards, as the system

approaches equilibrium. In time, as the encapsulation environment reaches hydration equilibrium, a more sustained release is enabled. A plateau is reached after 120 minutes as the drug appears to support a low release in the saline buffer. This behavior continues for the following two hours. The nanoparticles with poly(ethylene)glycol diacrylate show significant values of drug release of 75-79 %. The crosslinked structure could ensure a longer time for the drug release [34-36].

4. Conclusions

Silk fibroin-PEG nanoparticles were prepared by nanoprecipitation method. The nanoparticles were characterized in terms of morphological, physico-chemical and size distribution profile by SEM, FTIR, RAMAN and DLS. FTIR analysis revealed that the silk fibroin chemical modification was achieved. Physico-chemical investigation can conclude that PEG molecules approached the carbon double bond modified regions of silk molecules. They increased the nanoparticles hydrophilic nature with strong influences over encapsulation capacity, conformational changes, or crosslinked structure. Silk fibroin-PEG nanoparticles showed a good 5-FU encapsulation efficiency based on drug loading tests. As future perspectives, biological assessment of PEGylated SF nanoparticles will be done on specific tumor cell lines to optimize the system efficiency for cancer therapy.

Acknowledgements

DLS was possible due to European Regional Development Fund through Competitiveness Operational Program 2014-2020, Priority axis 1, Project No. P_36_611, MySMIS code 107066, Innovative Technologies for Materials Quality Assurance in Health, Energy and Environmental - Center for Innovative Manufacturing Solutions of Smart Biomaterials and Biomedical Surfaces – INOVABIOMED.

R E F E R E N C E S

[1]. *Y. Su, Z. Xie, G. B. Kim, C. Dong, J. Yang*, "Design strategies and applications of circulating cell-mediated drug delivery systems", in ACS Biomaterials Science & Engineering, **vol. 1**, no. 4, March 2015, pp. 201-217

[2]. *S. Grund, M. Bauer, D. Fischer*, "Polymers in Drug Delivery - State of the Art and Future Trends", in Advanced Engineering Materials, **vol. 13**, January 2011, pp. B61-B87

[3]. *O.P. Perumal, R. Panchagnula*, "Polymers in drug delivery", in Current Opinion in Chemical Biology, **vol. 5**, no. 4, September 2001, pp. 447-451

[4]. *G. Tiwari, R. Tiwari, B. Sriwastawa, L. Bhati, S. Pandey, P. Pandey, S.K. Bannerjee*, "Drug delivery systems: An updated review", in International Journal of Pharmaceutical Investigation, **vol. 2**, no. 1, January 2012, pp. 2-11

[5]. *S. Mukherjee, S. Ray, R.S. Thakur*, "Solid Lipid Nanoparticles: A Modern Formulation Approach in Drug Delivery System", in Indian Journal of Pharmaceutical Sciences, **vol. 71**, no. 4, July2009, pp. 349-358

[6]. *D. Liu, F. Yang, F. Xiong, N. Gu*, "The Smart Drug Delivery System and Its Clinical Potential", in Theranostics, **vol. 6**, no. 9, June 2016, pp. 1306–1323

[7]. *I. Brigger, C. Dubernet, P. Couvreur*, "Nanoparticles in cancer therapy and diagnosis", in Advanced Drug Delivery Reviews, **vol. 54**, no. 5, September 2002, pp. 631-651

[8]. *T.M. Saba*, "Physiology and Physiopathology of the Reticuloendothelial System", in Archives of Internal Medicine, **vol. 126**, no. 6, December 1970, 1031-1052

[9]. *G. Schmid*, Nanoparticles: From Theory to Application, 2nd, Completely Revised and Updated Edition, e-book, Wiley VCH Verlag, ISBN: 978-3-527-63236-7, 2011

[10]. *S. Sultana, M.R. Khan, M. Kumar, S. Kumar, M. Ali*, "Nanoparticles-mediated drug delivery approaches for cancer targeting: a review", in Journal of Drug Targeting, **vol. 21**, no. 2, February 2013, pp. 107-125

[11]. *S.D. Li, L. Huang*, "Nanoparticles evading the reticuloendothelial system: Role of the supported bilayer", in Biochimica et Biophysica Acta (BBA) – Biomembranes, **vol. 1788**, no. 10, October 2009, pp. 2259-2266

[12]. *A. Glišović, F. Vollrath*, Book Editor: Jürg Müssig, Mulberry Silk, Spider Dragline and Recombinant Silks in Industrial Applications of Natural Fibres: Structure, Properties and Technical Applications, John Wiley & Sons Ltd., 9780470660324, 2010

[13]. *A.R. Murphy, D.L. Kaplan*, "Biomedical applications of chemically-modified silk fibroin", in Journal of Materials Chemistry, **vol. 19**, June 2009, pp. 6443-6450

[14]. *H. Zhang, Ling-ling Li, Fang-yin Dai, Hao-hao Zhang, B. Ni, W. Zhou, X. Yang, Yu-zhang Wu*, "Preparation and characterization of silk fibroin as a biomaterial with potential for drug delivery", in Journal of Translational Medicine, **vol. 10**, no. 117, June 2012

[15]. *L.D. Koh, Y. Cheng, C.P. Teng, Y.W. Khin, X.J. Loh, S.Y. Tee, M. Low, E. Ye, H.D. Yu, Y.W. Zhang, M.Y. Han*, "Structures, mechanical properties and applications of silk fibroin materials", in Progress in Polymer Science, **vol. 46**, July 2015, pp. 86-110

[16]. *R.E. Marsh, R.B. Corey, L. Pauling*, "An investigation of the structure of silk fibroin", in Biochimica et Biophysica Acta, **vol. 16**, 1955, pp. 1-34

[17]. *E. Wenk, H.P. Merkle, L. Meinel*, "Silk fibroin as a vehicle for drug delivery applications", in Journal of Controlled Release, **vol. 150**, no. 2, March 2011, pp. 128-141

[18]. *B. Lotz, F.C. Cesari*, "The chemical structure and the crystalline structures of Bombyx mori silk fibroin", in Biochimie, **vol. 61**, no. 2, 1979, pp. 205-214

[19]. *F. Mottaghitalab, M. Farokhi, M.A. Shokrgozar, F. Atyabi, H. Hosseinkhani*, "Silk fibroin nanoparticle as a novel drug delivery system", in Journal of Controlled Release, **vol. 206**, May 2015, pp. 161-176

[20]. *C. Vepari, D.L. Kaplan*, "Silk as a Biomaterial", in Progress in Polymer Science, **vol. 32**, no. 8-9, 2007, pp. 991-1007

[21]. *K. Numata, D.L. Kaplan*, "Silk-based delivery systems of bioactive molecules", in Advanced Drug Delivery Reviews, **vol. 62**, no. 15, December 2010, pp. 1497-1508

[22]. *J. Magoshi, Y. Magoshi, S. Nakamura, N. Kasai, M. Kakudo*, "Physical properties and structure of silk. V. Thermal behavior of silk fibroin in the random-coil conformation", in Journal of Polymer Science: Polymer Physics Edition, **vol. 15**, September1977, pp. 1675-1683

[23]. *Z. Zhao, Y. Li, M.B. Xie*, "Silk Fibroin-Based Nanoparticles for Drug Delivery", in International Journal of Molecular Sciences, **vol. 16**, no. 3, March 2015, pp. 4880–4903

[24]. *T. Wongpinyochit, P. Uhlmann, A.J. Urquhart, F.Ph. Seib*, "PEGylated silk nanoparticles for anticancer drug delivery", in Biomacromolecules, **vol. 16**, no. 11, November 2015, pp. 3712-3722

[25]. *J.V. Jokerst, T. Lobovkina, R.N. Zare, S.S. Gambhir*, "Nanoparticle PEGylation for imaging and therapy", in Nanomedicine (Lond)., vol. 6, no. 4, June 2011, pp. 715-728

[26]. *T. Betancourt, J.D. Byrne, N. Sunaryo, S.W. Crowder, M. Kadapakkam, S. Patel, S. Casciato, L. Brannon-Peppas*, "PEGylation strategies for active targeting of PLA/PLGA nanoparticles", in Journal of Biomedical Materials Research Part A, vol. 91, no. 1, October 2009, pp. 263-276

[27]. *J. Wu, X. Xie, Z. Zheng, G. Li, X. Wang, Y. Wang*, "Effect of pH on polyethylene glycol (PEG)-induced silk microsphere formation for drug delivery", in Materials Science and Engineering C, vol. 80, November 2017, pp. 549-557

[28]. *C. Pinto Reis, R.J. Neufeld, A.J. Ribeiro, F. Veiga*, "Nanoencapsulation I. Methods for preparation of drug-loaded polymeric nanoparticles", in Nanomedicine: Nanotechnology, Biology, and Medicine, vol. 2, no. 1, March 2006, pp. 8-21

[29]. *H.Y. Kweon, S.H. Park, J.H. Yeo, Y.W. Lee, C.S. Cho*, "Preparation of Semi-Interpenetrating Polymer Networks Composed of Silk Fibroin and Poly(ethylene glycol) Macromer", in Journal of Applied Polymer Science, vol. 80, no. 10, June 2001, pp. 1848-1853

[30]. *M.R. Tudora, C. Zaharia, I.C. Stancu, E. Vasile, R. Trusca, C. Cincu,* "Natural silk fibroin micro- and nanoparticles with potential uses in drug delivery systems", in U.P.B. Sci. Bull., Series B, vol. 75, no. 1, 2013, pp. 43-52

[31]. *C. Andronescu, E.I. Biru, I.C. Radu, S.A. Garea, H. Iovu*, "Kinetics of benzoxazine polymerization studied by Raman spectroscopy", in High Performance Polymers, vol. 25, no. 6, February 2013, pp. 634-640

[32]. *E. Tanasa, C. Zaharia, A. Huditac, I.C. Radu, M. Costache, B. Galateanu*, "Impact of the magnetic field on 3T3-E1 preosteoblasts inside SMART silk fibroin-based scaffolds decorated with magnetic nanoparticles", in Materials Science & Engineering C, vol. 110, May 2020, 110714

[33]. *M. S. Zafar, K. H. Al-Samadani*, "Potential use of natural silk for bio-dental applications" in Journal of Taibah University Medical Sciences, vol. 9, no. 3, January 2014, pp. 171–177

[34]. *D.T. Pham, N. Saelim, R. Cornu, A. Béduneau, W. Tiyaboonchai*, "Crosslinked Fibroin Nanoparticles: Investigations on Biostability, Cytotoxicity, and Cellular Internalization", in Pharmaceuticals, vol. 13, no. 86, 2020

[35]. *D.-L. ZhuGe, L.-F. Wang, R. Chen, X.-Z. Li, Z.-W. Huang, Q. Yao, B. Chen, Y.-Z. Zhao, H.-L. Xu, J.-D. Yuan*, "Cross-linked nanoparticles of silk fibroin with proanthocyanidins as a promising vehicle of indocyanine green for photo-thermal therapy of glioma", in Artificial Cells, Nanomedicine, and Biotechnology, vol. 47, no. 1, December 2019, pp. 4293-4304

[36]. *I.C. Radu, A. Hudita, C. Zaharia, C. Negrei, G.T.A. Burcea Dragomiroiu, D.E. Popa, M. Costache, H. Iovu, M. Georgescu, O. Ginghina, B. Galateanu*, "Silk fibroin nanoparticles reveal efficient delivery of 5-FU in a HT-29 colorectal adenocarcinoma model in vitro", in Farmacia, vol. 69, no. 1, 2020, pp. 113-122.